Computational Materials Science 154 (2018) 472–480

Contents lists available at ScienceDirect

Computational Materials Science

journal homepage: www.elsevier.com/locate/commatsci

Origin of deflection of precipitates during interaction with a migrating twin boundary in magnesium alloys

F.X. Wang, B. Li*

Department of Chemical and Materials Engineering, University of Nevada, Reno, NV 89557, USA
Nevada Institute for Sustainability, University of Nevada, Reno, NV 89557, USA

ARTICLE INFO

Keywords:
Twin-precipitate interaction
Magnesium
Atomistic simulation

ABSTRACT

During interaction between a $Mg_{17}Al_{12}$ precipitate and a migrating $\{1\,0\,\bar{1}\,2\}$ twin boundary, a deflection on the precipitate has been reported and interpreted as a result of twinning shear. However, in the experimental reports, important features of twin boundaries that deviate from classical twinning behavior have been neglected. To better understand how such deflection is produced, in this work we performed atomistic simulations on interaction between precipitates and a moving twin boundary. Detailed analyses of lattice transformation during twinning, the evolution of the precipitate-matrix interfacial structure and the evolution of displacement of selected atoms of the precipitate were conducted. The results show that although the magnitude of twinning shear equals zero, deflection can still occur when the twin boundary is passing the precipitate. Such deflection is inversed during interaction as a result of relaxation to the precipitate caused by basal-prismatic transformation which generates a tensile strain along the *c*-axis of the parent. When the precipitate is partially engulfed by the twin, the portion in the parent and the portion in the twin experience different strain state, giving rise to the deflection which has nothing to do with the theoretical twinning shear.

1. Introduction

Magnesium (Mg) is the lightest structural metal which has a high specific strength due to its low density. Mg and its alloys have huge potential for engineering applications, for example, automotive industry to reduce the energy consumption [1–4]. Mg-Al-Zn alloys are the most common commercial materials, in particular, Mg-3Al-1Zn (AZ31) alloys have frequently been used as model alloys for fundamental research [5,6]. To increase the strength of these alloys, precipitation hardening is a main approach. Precipitates of metallic compounds produced through aging from solid solutions impede the movement of dislocations in the crystals [4,7–9]. Mg has a hexagonal close-packed (HCP) structure in which basal slip and $\{1\,0\,\bar{1}\,2\}\langle 1\,0\,\bar{1}\,1\rangle$ extension twinning are the two easy deformation modes in Mg [6,10–14]. Therefore, precipitates strengthening for Mg should consider the interactions of precipitates with both dislocations and migrating twin boundaries. However, precipitate hardening of Mg alloys is far less effective than that of Al alloys which has face center cubic (FCC) structure. This has been attributed to two possible reasons: (1) the dislocations do not effectively shear the precipitates because of the spacing is not small enough between the precipitates, thus, the strengthening effect is limited [15]; (2) The morphology of both discontinuous and continuous precipitates in Mg-Al-Zn Mg alloys are plate-like $Mg_{17}Al_{12}$ β-phase, and the primary orientation relationship with the matrix is the Burgers orientation relationship (OR), which is $(0\,0\,0\,1)_{Mg}\|(0\,1\,1)_P$, $[2\,\bar{1}\,\bar{1}\,0]_{Mg}\|[1\,\bar{1}\,1]_P$ [7,16–19]. The precipitate plates are parallel to the basal plane of the matrix, and thus less effective to block the basal slip which is the easiest deformation mode in Mg alloys [20].

Interactions between precipitates and dislocation slip have been studied through both computational simulations and experiments. Liao et al. [21,22] studied the interactions of $Mg_{17}Al_{12}$ β-phase with basal and prismatic slip in Mg using molecular dynamic (MD) simulations. They found that when a basal dislocation impinges on a precipitate, it can pass the precipitates without generating a dislocation loop or cutting into the precipitate. In contrast, a prismatic dislocation can shear through the particles. By using the Orowan looping mechanism, Robson et al. [8,9,23] calculated the hardening effect from precipitation [20]. They showed that the shape and habit plane of the precipitate have an effect on the mechanical asymmetry in Mg alloys. Rod-like precipitates along the *c*-axis are more effective impeding dislocation slip by increasing the critical resolved shear stress (CRSS) of dislocation slip, than plate-like plates that are parallel to the basal plane.

In addition to precipitate/dislocation interaction, interaction

* Corresponding author at: Department of Chemical and Materials Engineering, University of Nevada, Reno, NV 89557, USA.
E-mail address: binl@unr.edu (B. Li).

https://doi.org/10.1016/j.commatsci.2018.08.020
Received 12 June 2018; Received in revised form 9 August 2018; Accepted 10 August 2018

between precipitates and TBs may play another important yet less understood role in the hardening behavior of Mg alloys and other HCP metals. In classical twinning theory, TB migration is generally mediated by twinning dislocations on the twinning plane [11,12]. The twinning dislocations generate the required simple shear which is homogeneously distributed over consecutive twinning planes, resulting in a shape change. It can be expected that precipitates will interact with migrating TBs [8,24,25]. Gharghouri et al. [25] performed transmission electron microscopy (TEM) observations on interaction between a $\{1\,0\,\bar{1}\,2\}\langle 1\,0\,\bar{1}\,1\rangle$ twin and $Mg_{17}Al_{12}$ precipitates. They found that the $Mg_{17}Al_{12}$ particles can be totally engulfed by the twin without being sheared. Experiments also observed that large precipitate can entirely arrest twin growth [25], and a precipitate can be sheared inside a twin [26,27]. Recently, Liu et al. [28] studied twin-precipitate interaction using in-situ TEM on micro-pillars. They observed that the dispersed particles (rods or basal plates) are ineffective in suppressing TB migration. Wang et al. [29] also observed similar behavior that precipitates in a Mg-5Zn alloy cannot suppress twinning during micropillar compression. Li et al. [30] simulated interaction between a $\{1\,0\,\bar{1}\,2\}$ twin and a $Mg_{17}Al_{12}$ precipitate using atomistic simulations, and showed that the particle was not sheared as the TB passed through, and twin growth was not mediated by twinning dislocations. Recently, Li and Zhang showed that the magnitude of $\{1\,0\,\bar{1}\,2\}$ twinning shear cannot be any finite value but zero by using lattice correspondence analysis [31], which is able to account for the anomalous properties of this particular twinning mode.

Fig. 1 shows an example of twin-precipitate interaction reported by Geng et al. [32]. The TB is passing the precipitate and a deflection of the precipitate can be observed. This deflection was interpreted as a result of twinning shear. In this figure, the parent basal plane was indicated by the white dashed line. Although the misorientation angle is ~86°, if we add the trace of the $\{1\,0\,\bar{1}\,2\}$ twinning plane (the yellow line) to this micrograph, immediately, two important features can be observed. First, the TB is incoherent and departs from the twinning plane. Second, although the TEM micrograph was taken right on the zone axis, the TB appears to be a rather wide band of extinction of contrast which clearly indicates the TB is not edge-on as it should be. This implies that the TB is not sharing the same zone axis with the twinning plane, which should not happen in classical twinning theory. Thus, a homogeneous simple shear, which is required in classical twinning, cannot occur on the twinning plane or on the TB. Then a question arises: what causes the deflection of the precipitate?

To answer this question, in this study, we closely examine how a plate-like $Mg_{17}Al_{12}$ precipitate interacts with a moving $\{1\,0\,\bar{1}\,2\}\langle 1\,0\,\bar{1}\,1\rangle$ TB on the atomic scale when a tensile load is applied along the *c*-axis of the parent crystal. Lattice correspondence analysis is used to analyze the lattice transformation such that the interaction mechanism can be better resolved and understood. The results provide new insight on the deformation behavior of Mg-Al-Zn alloys.

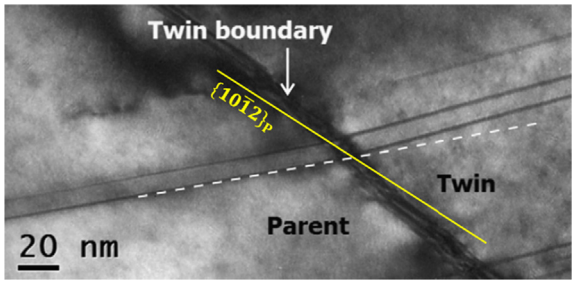

Fig. 1. The observed deflection of a precipitate when a twin boundary (TB) is passing (with permission of Elsevier) [32]. Notably the TB departs from the twinning plane (the solid yellow line) and not edge-on although the misorientation angle was ~86° and the TEM image was taken right on the zone axis. (For interpretation of the references to color in this figure legend, the reader is referred to the web version of this article.)

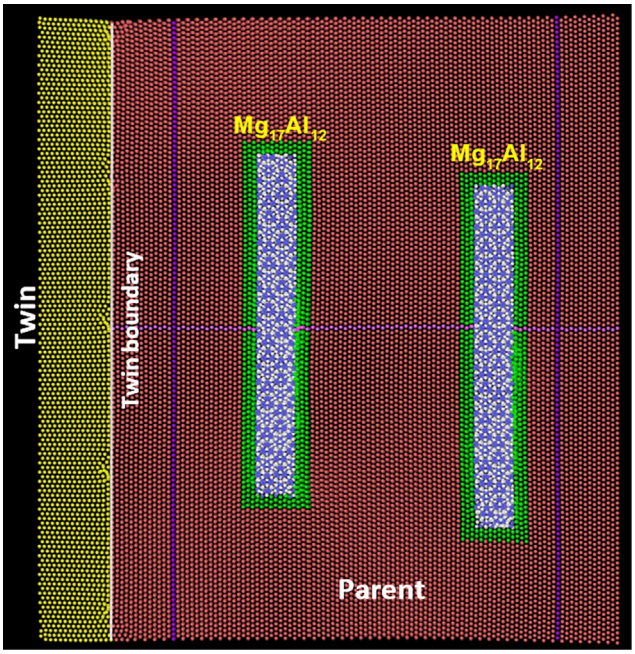

Fig. 2. The relaxed configuration of the atomistic simulations. Two plate-like $Mg_{17}Al_{12}$ precipitates (Mg in white; Al in blue) were embedded inside the Mg parent (in red). A $\{1\,0\,\bar{1}\,2\}$ twin shown in yellow. In the parent, a prismatic plane (in pink) and two basal planes (in purple) were pre-selected for structural analysis. Three layers of Mg atoms of the parent at the $Mg/Mg_{17}Al_{12}$ interface were colored in green. The color patterns were retained throughout the simulations such that structural evolution can be better analyzed. (For interpretation of the references to color in this figure legend, the reader is referred to the web version of this article.)

2. Simulation method

The atomistic simulation was performed by using XMD molecular dynamics simulation package. Embedded atom method (EAM) [33] interatomic potentials developed by Liu et al. [34,35] was used for the simulations. The visualization tool Ovito [36] was used for analyzing the simulation data.

The initial simulation system was constructed as shown in Fig. 2. The dimension of the system is 25 × 32 × 35 nm which comprises a total number of 1,237,500 atoms. A pre-existing TB was constructed. The atoms of the $\{1\,0\,\bar{1}\,2\}$ twin are colored in yellow, and those atoms of the parent are colored in red. The TB is a basal/prismatic interface that has been observed extensively in TEM and simulations [31,37]. In low magnification TEM observations [32], TBs tend to be close to the twinning plane due to their lower TB energies. But in high resolution TEM (HRTEM) observations [31], TBs are still composed of nanoscale basal/prismatic interfaces. Two plate-like β-phase precipitates were placed in the Mg matrix. Each precipitate has a thickness ~2.0 nm with an aspect ratio ~10. The plate plane of the precipitates is parallel to the basal plane of the parent. The left precipitate is located about 8 nm away from the TB. The distance between the bottom surface of the left precipitate and that of the matrix is about 8 nm. For the right precipitate, it resides about 20 nm away from the TB, and the distance between the bottom surface of the right precipitate and that of the matrix is about 6 nm. The orientation relationship between the precipitates and the matrix satisfies the Burgers OR. We color three layers of matrix Mg atoms which are at immediate vicinity to the precipitates. The structure of these interfacial layers will be analyzed in great detail such that a high clarity can be achieved.

Additionally, in the Mg parent, atoms on a double-layered or

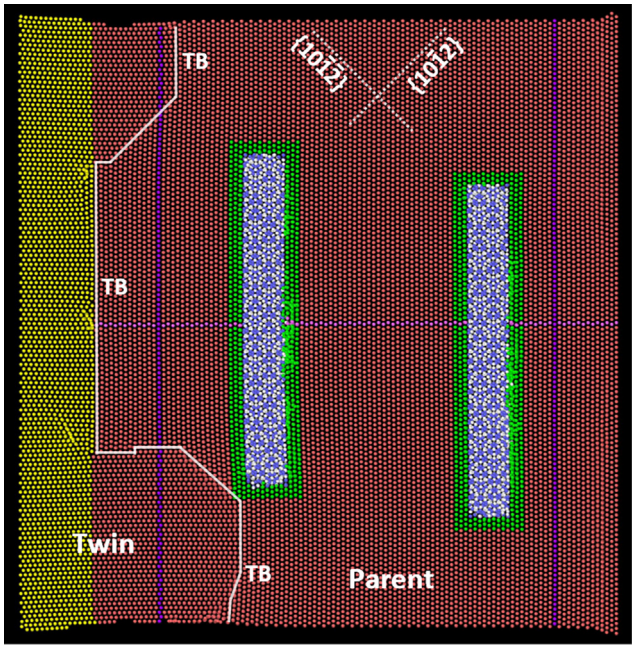

Fig. 3. As the tensile strain increases, the twin boundary (TB, indicated by the white line) starts to migrate toward the parent. Note that the moving TB does not coincide with the {1 0 $\bar{1}$ 2} or {10$\bar{1}$2} twinning planes. At this point the TB has not impinged on the left precipitate, but the precipitate is already slightly bent due to the elastic strain.

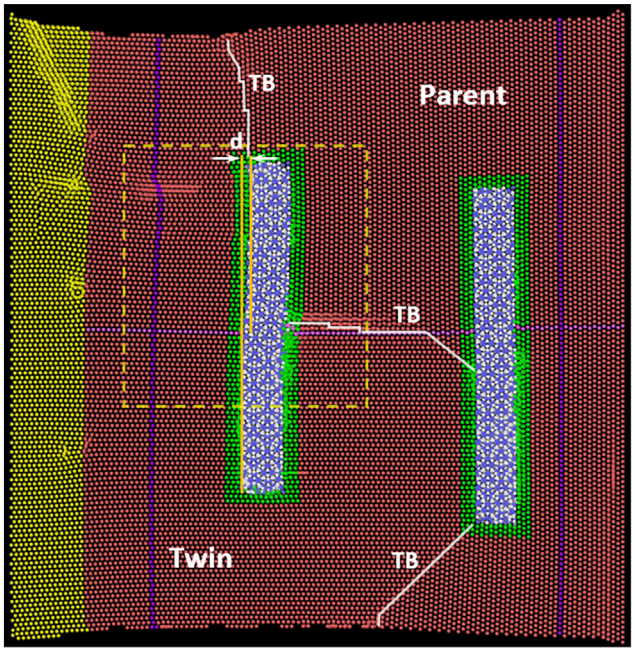

Fig. 4. Interaction between the precipitate and the TB. The TB is halfway through engulfing the left precipitate. During interaction, a deflection on the precipitate can be seen, as indicated by the displacement of d, i.e. the top and the bottom half of the precipitate are displaced non-uniformly.

corrugated prismatic plane are colored in pink, whereas atoms on a single-layered basal plane are colored in purple. The color patterns of the system were maintained throughout the simulations, such that any structural evolution in these colored regions can be definitively revealed and analyzed.

Free surface conditions were applied to the whole system. During the simulation, the temperature was maintained constant at 10 K. The time step size was 3.0 fs. Before the tensile strain was applied, the system was relaxed for 20,000 time steps (60 ps). During straining, the right surface was fixed, and the left surface was moved at a constant rate corresponding to a strain rate of $\sim 2 \times 10^8\,s^{-1}$.

3. Results

As the tensile strain increases, the pre-existing TB starts migrating toward the parent, and this process is shown in Fig. 3. The TB migration begins at both the top and bottom surface of the simulation system, as indicated by the white lines. The middle section of the TB remains still. Notably, the migrating TB sections evolve into a mixture of segments of basal/prismatic interfaces, i.e. incoherent TB, and segments parallel to the {1 0 $\bar{1}$ 2} twinning plane, i.e. coherent TB. By incoherent, we mean that the TB does not match the {1 0 $\bar{1}$ 2} twinning plane, and it can be seen that the TB can be either parallel or perpendicular to the basal plane of the matrix. The {1 0 $\bar{1}$ 2} twinning plane should make an angle of 43.15° with the parent basal plane, theoretically. If we closely examine the purple atoms that are pre-selected in one of the parent basal plane, it can be clearly seen that the originally flat parent basal plane now partially transforms to a zigzag prismatic plane. The already transformed segments are parallel to the untransformed segment. At this point, the TB is approaching the left precipitate but not in contact yet. However, we can observe that the precipitate is already slightly bent, due to the elastic strain.

As the tensile strain further increases, the TB impinges upon the precipitate. However, the impingement does not hinder the twin growth. As seen in Fig. 4, as the parent is transforming into the twin, the precipitate is gradually surrounded by the twin while the TB propagates into the parent. Note the TB is still composed of basal/prismatic segments, nearly coherent segments and a few one-layer basal/prismatic steps. The bottom half of the precipitate is now embedded inside the twin. Also, as the TB moves up along the precipitate/matrix interface, the bottom half of the precipitate, which was slightly bent (Fig. 3), now recovers almost to its straight position. However, the overall shape of the precipitate remains distorted, in the sense that the top half of the precipitate is displaced to the right in reference to the bottom half. Two solid, yellow lines are drawn to indicate the uneven displacement from top to bottom which causes a deflection on the precipitate.

Eventually, the left precipitate was totally engulfed by the twin as the TB migrates and impinges upon the second precipitate, as shown in Fig. 5. It is obvious that the engulfed precipitate remains deflected, however, the degree of deflection is less than that in Fig. 4 as denoted by the reduced value of d, indicating that as the TB is moving up along the precipitate/matrix interface, the precipitate is recovering from the deflection. The TB is still composed of nearly coherent interface and incoherent basal/prismatic interface while migrating.

As the TB migrates far away from the engulfed precipitate, the deflection is largely recovered, and the shape of the precipitate is almost restored to the straight position (Fig. 6). Careful examination reveals that the thickness of the precipitate is slightly increased, but the height is slightly reduced. This is due to the fact that when a tensile strain is applied along the *c*-axis of the parent, an extension is created along the *c*-axis, but a contraction is also created simultaneously in the direction perpendicular to the *c*-axis. This is the very reason why {1 0 $\bar{1}$ 2} twinning mode is oftentimes called “extension twinning”. This effect can be clearly observed from the cosmetic change of the top and bottom surfaces of the system.

4. Analysis and discussion

4.1. Inversion of deflection during TB migration

Before we analyze precipitate-TB interaction, it is necessary to examine the mechanism of {1 0 $\bar{1}$ 2} twinning. The analysis is shown in Fig. 7a–c which clearly presents how the parent lattice is transformed to

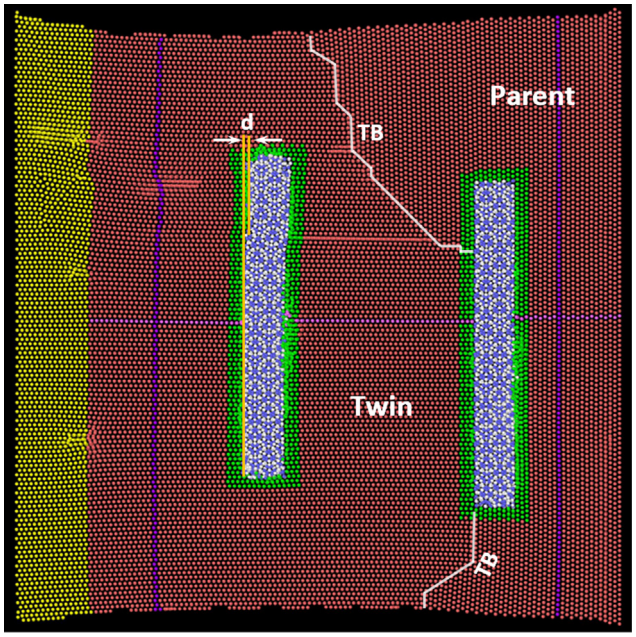

Fig. 5. The TB entirely passes through the left precipitate. Note that the left precipitate remains deflected after the TB no longer in contact with the precipitate, but the deflection is not as large as in Fig. 4.

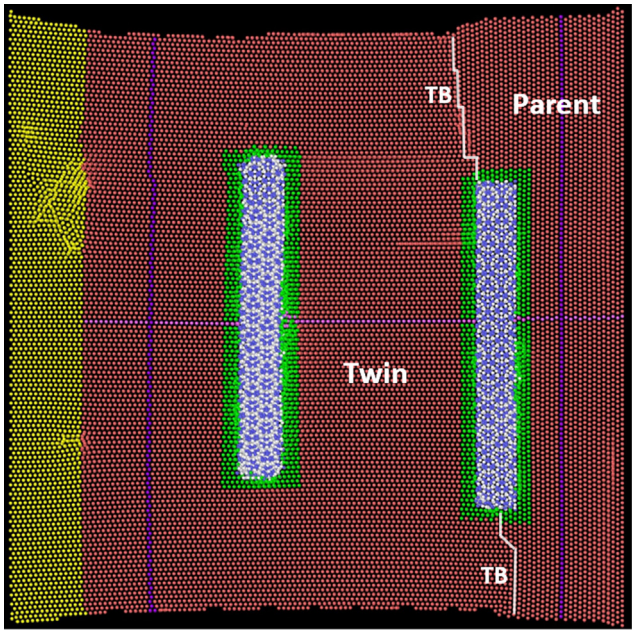

Fig. 6. The TB interacts with the precipitate on the right. Note that the deflection on the left precipitate almost disappears. The width of the left precipitate slightly increases.

the twin lattice. Fig. 7a shows a magnified view of the pre-selected parent basal plane (in purple) and the parent prismatic (in pink), and the pre-selected three-layer parent basal planes (in green) that are in contact with the precipitate before straining. It can be clearly seen that, when the TB is traversing through the parent, the initially single-layered basal plane of the parent now becomes the double-layered prismatic plane of the twin; whereas the initially double-layered prismatic plane of the parent now becomes the single-layered basal plane of the twin (Fig. 7b). An important characteristic of this lattice transformation is that, the green atoms which are initially the basal planes of the parent, are also all transformed to the prismatic planes of the twin

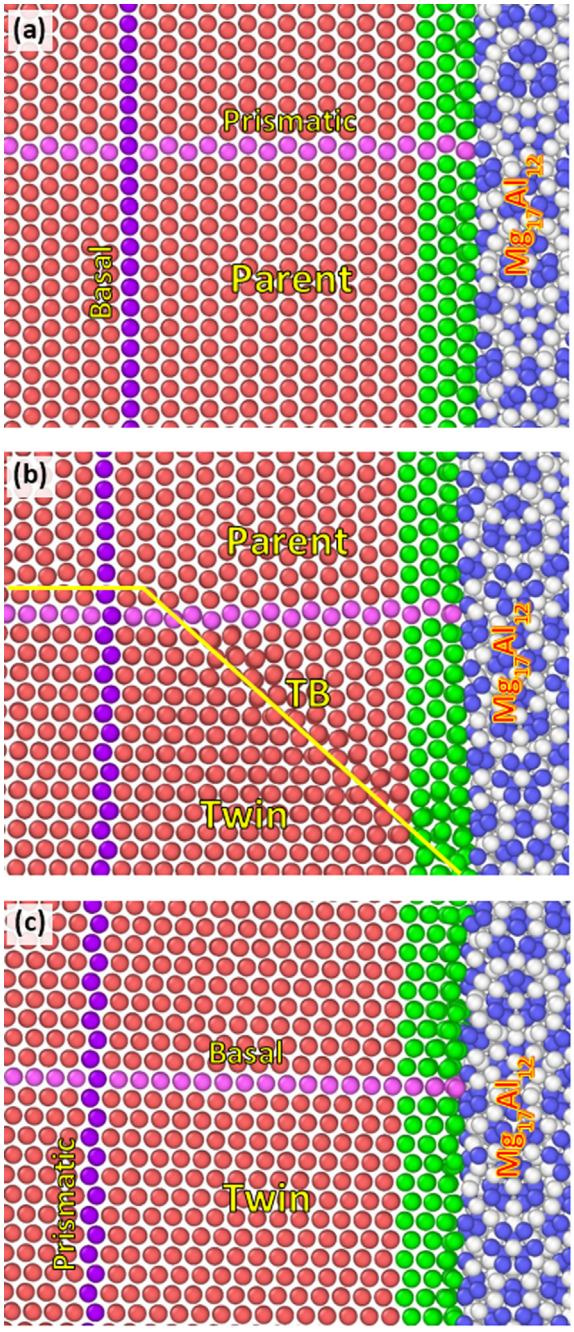

Fig. 7. Lattice transformation analysis during $\{1\,0\,\bar{1}\,2\}$ twinning. (a) A selected area of the parent after relaxation. The parent basal is a flat atomic plane and the prismatic is a rumpled one. (b) When the TB migrates toward the precipitate, the flat basal turns into the rumpled prismatic, whereas the rumpled prismatic turns into the flat basal. (c) After the selected area is totally twinned, the pink prismatic plane of the parent transforms to the basal plane of the twin. The purple basal plane of the parent transforms to the prismatic plane of the twin. (For interpretation of the references to color in this figure legend, the reader is referred to the web version of this article.)

(Fig. 7c). This suggests that the strength of the precipitate-matrix interface is not strong enough to prevent the green basal planes from being transformed by the twinning process. As a result of twinning, the initial Burgers OR is no longer satisfied. A recent calculation [38] of interfacial energies between Mg and $Mg_{17}Al_{12}$ shows that, the Burgers OR produces a low energy, semi-coherent interface; after twinning, the interfacial energy is almost doubled and the interfacial structure becomes more disordered.

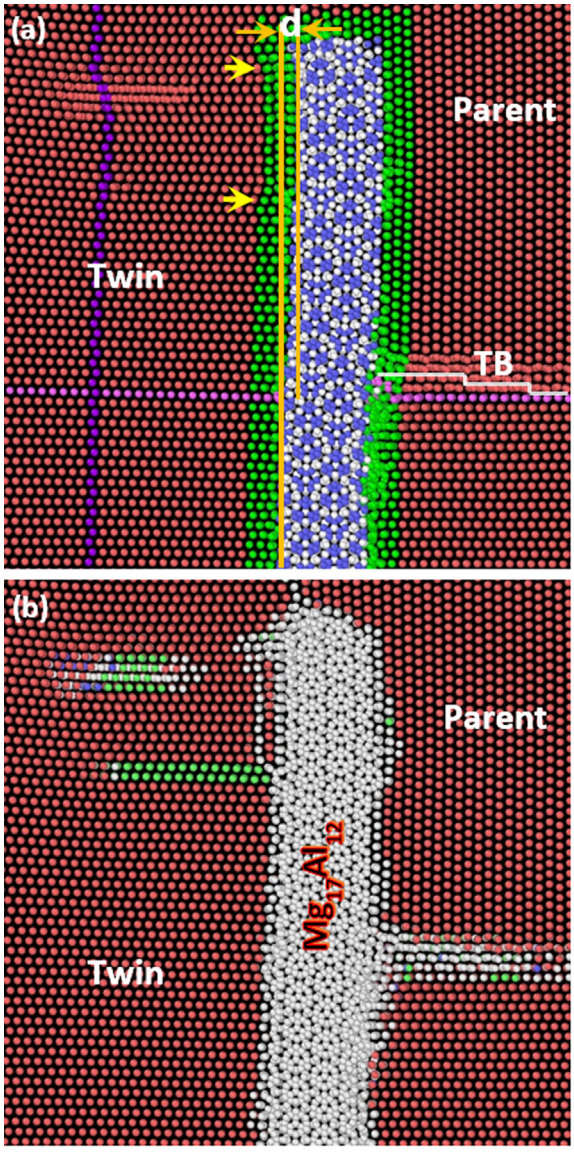

Fig. 8. (a) An enlarged view of the deflected precipitate when the TB is interacting with it. To the green atoms on the left side, two shear steps can be seen, as indicated by the two yellow arrows. (b) Common neighbor analysis of the structure in Fig. 8a. HCP structure is colored in red and FCC is in green which indicates the presence of basal stacking faults. Structures other than HCP and FCC are colored in white and blue. (For interpretation of the references to color in this figure legend, the reader is referred to the web version of this article.)

Because the initial misorientation angle between the parent and the twin equals 90° (Fig. 2) rather than the theoretical value of 86.3°, the $\{1\,0\,\bar{1}\,2\}$ twinning planes of the parent and the twin do not coincide. This indicates that the invariant plane strain (IPS) condition for deformation twinning [31,39] is not satisfied. The IPS condition requires that (1) the twinning plane be structurally undistorted during twinning; (2) the actual TB coincide with the twinning plane. Extremely incoherent TBs in $\{1\,0\,\bar{1}\,2\}$ twinning have been observed extensively in experiments and simulations [31,38,39]. For a typical example, Liu et al. [28] revealed with in-situ TEM observations that the misorientation angle can indeed equal 90° when a single crystal Mg specimen was deformed in tension along the *c*-axis. The 90° misorientation angle excludes any possible twinning shear during the twinning process [31]. Then why the precipitate was deflected by the moving TB?

Next, we magnify the boxed area in Fig. 4, and the structure is shown in Fig. 8a. The deflection can now be better resolved. As indicated by the two yellow arrows, two shear steps can be seen from the green atoms, indicating that dislocation slip in the matrix occurred during deformation. It is necessary to analyze the nature of these matrix dislocation, such that the real cause of the deflection on the precipitate can be determined. Fig. 8b shows common neighbor analysis [40,41] of dislocations and stacking faults. Atoms in perfect HCP structure are shown in red, and atoms of FCC structure are shown in green. Atoms of other structures are shown in white and blue, for example, atoms at the dislocation core and the precipitates. It can be seen that, basal dislocations are activated during twinning, despite that the Schmid factor of the basal slip is close to zero.

The nucleation process of the basal dislocations at the TB is shown in Fig. 9a–d. It is clear that the migration of the TB in the simulation completely departs from the classical planar growth which should be exactly on the twinning plane mediated by twinning dislocations. In Fig. 9a, two segments of TBs are approaching each other, and the region in between has not been twinned. In the boxed region, green atoms, which are basal stacking faults, can be observed. As the two TB segments approach each other, another basal dislocation is formed, as indicated by the dashed box in Fig. 9b. Eventually, the two TB segments merge, and two fully developed basal stacking faults and the associated partial dislocations can be seen (Fig. 9c–d). The basal dislocations disappear at the matrix-precipitate interface as they glide and reach the interface. After twinning, the basal plane of the twin is now nearly parallel to the loading direction. Thus, the Schmid factor of the basal dislocations is nearly zero. Also, because the basal dislocations are mostly edge-type, the shear stress on the basal plane from the stress field of dislocations is nearly zero. Therefore, these basal dislocations have little effect on the deflection of the precipitate.

To further reveal how the precipitate is deflected during interaction with the migrating TB, we provide a series of images of the precipitate in time sequence, as shown in Fig. 10a–f. It can be observed that during precipitate-TB interaction, the shape of the precipitate constantly changes as the TB progressively engulfs it. Several interesting features can be seen. First, from Fig. 10c–d, the deflection of the precipitate is inversed. After the inversion, as the TB is moving upward and more and more of the precipitate is being engulfed by the twin, the deflection reduces. After the precipitate is entirely engulfed and most of the parent is twinned, the deflection is largely recovered. Notably, the precipitate becomes slightly wider (Fig. 10f) due to the extension along the parent *c*-axis produced by $\{1\,0\,\bar{1}\,2\}$ twinning.

To better understand the evolution of the shape of the precipitate, we selected three atoms in the top, middle and bottom of the precipitate, and recorded the positions of these atoms versus simulation time. The displacements of these three atoms were plotted and shown in Fig. 11. Each of the displacement curves presents three stages. First, a constant increase in displacement despite the undulation. This corresponds to the elastic deformation when the whole system is being stretched in tension along the *c*-axis of the parent. Second, a sudden drop in displacement. This corresponds to the initiation of TB migration, which gives rise to a relaxation in the system. Third, the displacement increases again, and this corresponds to the elastic deformation after the relaxation. Now the behavior of deflection on the precipitate can be well understood. For the bottom half of the precipitate, because TB migration first initiates near the top and bottom surfaces of the system (Fig. 3) and migrates faster toward the precipitate in the bottom half (Fig. 4), the selected atom in the bottom experiences the relaxation to the elastic strain when the TB approaches the precipitate. This relaxation causes the bottom half of the precipitate shifts in the direction opposite to the external strain (Fig. 3). This is the initial deflection observed on the precipitate (Fig. 10b). As the TB in the lower half of the system migrates, interacts and then partially engulfs the precipitate, the elastic strain picks up again because the twinned region is now being strained by the external load. This causes the displacement of the atoms in the bottom quickly increases as the external strain increases. In contrast, for the selected atom in the middle, the

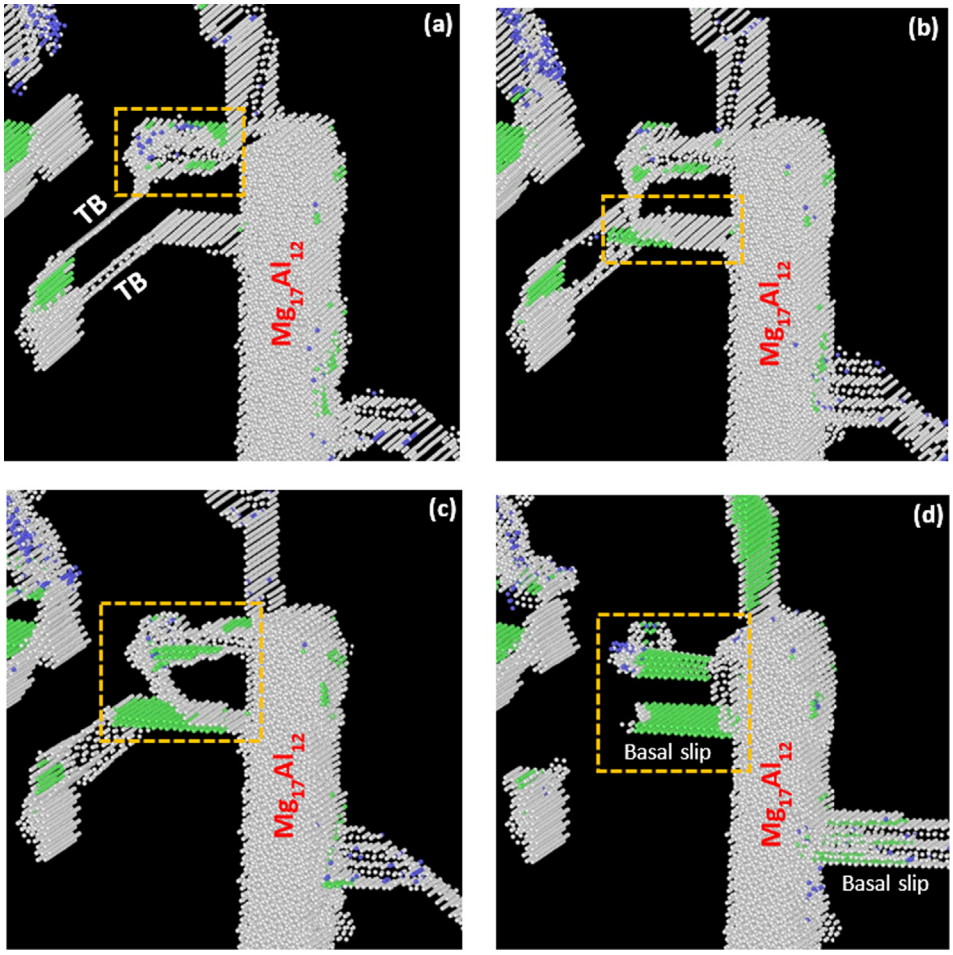

Fig. 9. Nucleation of basal slip at the TB. (a) Basal dislocations are nucleated at the TB (indicated by the dashed box). (b) Another basal dislocation is activated when the two TBs join. (c) The basal dislocations move toward the precipitate. (d) Fully developed basal stacking faults of the basal dislocations. Meanwhile, basal slip also nucleate at the right Mg/precipitate interface.

relaxation lags behind because TB migrates faster in the loading direction and slower in the vertical direction. This behavior is seen in the red[1] curve in Fig. 11. When the blue curve and red curve cross over, i.e. the displacement of the bottom atom is increasing whereas the displacement of the middle atoms is rapidly decreasing, this corresponds to the inversion of the deflection of the precipitate (Fig. 10c–d). For the selected atoms in the top, the relaxation further lags behind (the green curve). After the precipitate is entirely engulfed by the twin, the displacement of the top atom picks up again and this corresponds to the recovery of the deflection (Fig. 10e).

The above analysis reveals that the deflection on the precipitate when a migrating TB is interacting with the precipitate is purely a result of sequential elastic deformation – relaxation by twinning – elastic deformation. No twinning shear is involved. In the following, we discuss in detail how these events interplay during precipitate-TB interaction.

4.2. Absence of twinning shear

To explain the increase in stress for twinning with increasing volume fraction of $Mg_{17}Al_{12}$ in Mg alloys, Barnett et al. treated a growing twin as a "super dislocation loop" [42,43]. This idea is similar to the proposition of "geometrically necessary twins" by Sevillano [44] who treated a twin as a "super dislocation" by assuming a homogeneous simple shear on the twinning plane. As seen from the extensive experimental and simulation reports, $\{1\,0\,\bar{1}\,2\}$ TBs are extremely incoherent and thus a homogeneous simple shear is unlikely to happen on the twinning plane. Because the Orowan loop mechanism fails to provide a good explanation to the precipitation hardening on twinning, Robson [45] considered the effect of precipitates on the internal stress during twin propagation in Mg. The Eshelby model [46–48] was used to evaluate the internal stress for an embedded precipitate with different shape and habit plane. The misfit strain and stresses around the particle were calculated. The strain incompatibility between the twin and the precipitate produced a back stress, and this misfit strain was accommodated by the deformation of matrix and the elastic deformation of the precipitate. More recently, Fan et al. [49] investigated the precipitate hardening effect in terms of precipitate geometry on twinning via atomistic simulations by assuming twinning dislocations on the highly incoherent TBs.

As shown in the initial configuration of the system (Fig. 2), the misorientation angle equals 90°. Thus, no homogeneous simple shear should occur on the theoretical $\{1\,0\,\bar{1}\,2\}$ twinning plane. This can also be seen from the extremely incoherent actual TB in the simulations. The pre-selected and colored parent basal and prismatic planes (Figs. 3 and 4) corroborate that, the twinning process is accomplished by the transformation of parent basal to twin prismatic and parent prismatic to twin basal. This lattice transformation prohibits a homogeneous simple shear from occurring on the twinning plane. As seen in Figs. 3 and 7, after lattice transformation, the parent basal is parallel to the twin

[1] For interpretation of color in Figs. 9–11, the reader is referred to the web version of this article.

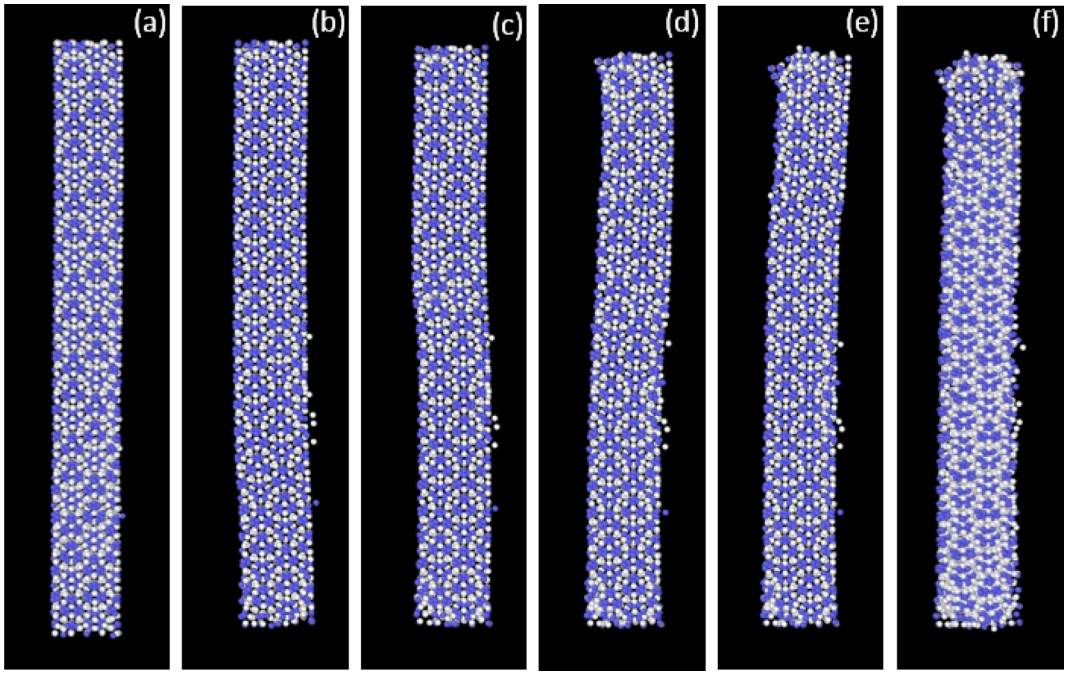

Fig. 10. Evolution of the shape of the precipitate during interaction with the TB. (a) The relaxed structure of the precipitate before straining. (b) The precipitate is deflected before in contact with the TB. (c) The TB is halfway through the precipitate. (d) The deflection is inversed as the strain further increases. (e) The deflection is being recovered as the TB is engulfing the precipitate. (f) The precipitate largely recovers after the TB entirely passes through. Note the precipitate becomes slightly wider due to the extension along the parent *c*-axis produced by $\{1\,0\,\bar{1}\,2\}$ twinning.

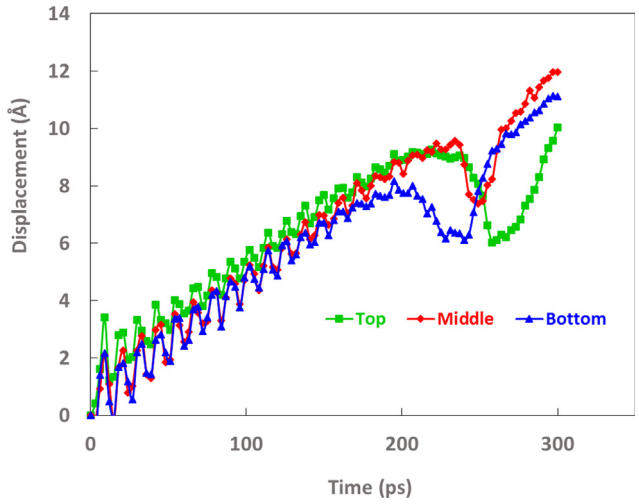

Fig. 11. Evolution of the displacements along the loading direction of three atoms which are at the top, middle and bottom of the precipitate. The time at which the displacement starts to drop indicates relaxation caused by $\{1\,0\,\bar{1}\,2\}$ twinning. These atoms reach the minimum at different times.

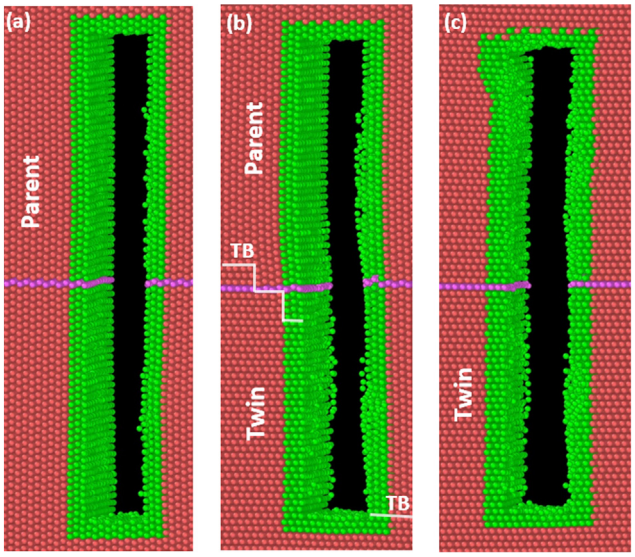

Fig. 12. Structural evolution of the matrix when the precipitate is removed. (a) The relaxed structure before straining. (b) When the TB is interacting with the precipitate. No trace of twinning dislocations can be identified on the wall of green atoms. (c) After the TB passes through and the precipitate springs back, no trace of twinning dislocations can be observed. (For interpretation of the references to color in this figure legend, the reader is referred to the web version of this article.)

prismatic and the parent prismatic is parallel to the twin basal, thus, the magnitude of twinning shear must be zero, because any non-zero twinning shear would destroy the two parallelisms [31].

To further reveal the nature of zero twinning shear, we highlight the pre-selected green atoms of the parent and focus on the interfacial structure (Fig. 12). In these plots, the precipitate is removed such that the inner surfaces of the green frame of the matrix are shown. Before straining (Fig. 12a), the exposed vertical surface is the basal plane of the matrix. When twinning is happening (Fig. 12b), the basal plane is transformed to the prismatic plane of the twin, however, the surface remains flat despite the double-layered structure of the prismatic plane. In other words, no shear strain produced by a homogeneous simple shear can be observed. The theoretical magnitude of twinning shear equals 12.9% which is fairly large. Such a large magnitude of twinning shear would produce an observable shear strain on the green surface. After the precipitate is entirely engulfed by the twin (Fig. 12c), the deflection of the precipitate is largely recovered, and no shear strain can be observed as well.

$\{1\,0\,\bar{1}\,2\}\langle 1\,0\,\bar{1}\,\bar{1}\rangle$ twinning is oftentimes called “extension twinning” in the literature. For HCP metals with c/a ratios (λ) less than $\sqrt{3}$, this twinning mode is activated when a tensile load is applied along the *c*-

axis of the parent or when a compressive load is applied perpendicular to the *c*-axis; in contrast, it is not activated when an external load is applied in reversed directions [10]. This unidirectionality stems from the fact that this particular twinning mode generates an extension along the *c*-axis when the parent lattice is reoriented by ~90° around the zone axis of the parent and twin basal planes [10,31,37]. After twinning, the parent basal is transformed to the twin prismatic. But, the interplanar spacing of the prismatic plane equals $\frac{1}{2}\sqrt{3}a_0$ (a_0 is the lattice parameter). Compared to the original interplanar spacing of the basal plane which equals $\frac{1}{2}\cdot\lambda\cdot a_0$, an increase in the interplanar spacing is produced by twinning along the *c*-axis of the parent. The increase equals:

$$\varepsilon = \frac{\sqrt{3}a_0 - \lambda\cdot a_0}{\lambda a_0} = \frac{\sqrt{3}-\lambda}{\lambda} \quad (1)$$

Thus, when $\lambda < \sqrt{3}$, a positive, tensile strain is produced along the *c*-axis of the parent. This conclusion seems to be the same as the well-known "$\sqrt{3}$ criterion" proposed by Yoo [50] which is based on the theoretical twinning shear reverses its sign at $\lambda = \sqrt{3}$. Our analysis is based on the lattice correspondence which shows no homogeneous simple shear should be involved. Thus, when $\{1\ 0\ \bar{1}\ 2\}$ twinning occurs, due to the extension produced along the *c*-axis of the parent by lattice reorientation, a relaxation occurs when the TB starts migrating (Fig. 11). Such a strain accommodation process is fundamentally different from a plastic strain generated by dislocation glide on the slip plane which produces microscopic displacements in the crystal that induce either a tensile or a compressive strain macroscopically.

Unlike other known twinning modes in FCC, BCC and HCP metals, $\{1\ 0\ \bar{1}\ 2\}\langle 1\ 0\ \bar{1}\ \bar{1}\rangle$ twinning mode does not have a unique value of misorientation angle [51–53]. For Mg, the misorientation angle can deviate from 90° for a few degrees [39]. The theoretical misorientation angle equals 86.3°, which produces nearly coherent, low TB energy structures [54]. The multiple values of the misorientation angle preclude any possibility of a homogeneous simple shear on the twinning plane [55,56]. According to the classical twinning theory, a twinning mode can only have a unique value of magnitude of twinning shear. Li and Ma [37] first reported that this twinning mode is accomplished by atomic shuffling and no twinning dislocations should be involved. More recently, Li and Zhang [31] showed that the lattice correspondence analysis based on the assumption in the classical twinning theory that the twinning plane must be an invariant plane gives rise to exactly the lattice transformation shown in Fig. 7. They further showed that given such a lattice transformation, the $\{1\ 0\ \bar{1}\ 2\}$ twinning plane cannot remain invariant during twinning. Thus, no homogeneous simple shear can happen on the twinning plane. When the misorientation angle deviates from 90° for a few degrees, the generated tensile strain along the *c*-axis is slightly (less than 1%) smaller than the case of 90°. No matter what misorientation angle is, the contribution to the tensile strain comes from Eq. (1), rather than from the "twinning shear" which equals zero irrespective of the misorientation angle.

If there were a twinning shear acting on the precipitate, such a twinning shear would have to be carried by twinning dislocations on consecutive twinning planes. If these twinning dislocations could not cut into the precipitate, we would expect to observe dislocation loops around the precipitate, but this is not the case in experimental observations. If the twinning dislocations could cut into the precipitates, the precipitate would be deformed permanently, but this is not the case either. In fact, in experimental observations, such deflections can always be fully recovered [25,57].

The above analysis well explains how and why a precipitate deflects when a migrating TB is interacting with it. The portion of a precipitate that is embedded inside the parent and the portion that is embedded inside the twin experience different strain state. For the portion that is engulfed by the twin, an extra tensile strain component produced by the lattice reorientation is acting on it; but for the portion that is still embedded inside the parent, such a component is absent. This difference leads to the deflection of the precipitate during interaction. After the precipitate is completely engulfed by the twin, the difference in strain state vanishes and the deflection is recovered consequently. Although such a deflection can be most conveniently and intuitively interpreted as a result of twinning shear and the resultant twinning dislocations inside the framework of the classical twinning theory, the non-classical nature of this particular twinning mode should not be neglected, as reported in Fig. 1 and many other experimental observations. The unique twinning mechanism for $\{1\ 0\ \bar{1}\ 2\}\langle 1\ 0\ \bar{1}\ \bar{1}\rangle$ mode can provide a better understanding of the deformation behavior of Mg and Mg alloys.

5. Conclusions

In this work, we performed atomistic simulations to investigate the origin of deflection of a $Mg_{17}Al_{12}$ precipitate during interaction between the precipitate and a moving $\{1\ 0\ \bar{1}\ 2\}$ TB. Following conclusions can be reached:

(1) A precipitate can be entirely engulfed by a twin. During precipitate-TB interaction, no twinning shear and twinning dislocation are involved.
(2) Deflection occurs during precipitate-TB interaction, although the magnitude of twinning shear equals zero. Such deflection is a result of lattice reorientation which produces a tensile strain along the *c*-axis of the parent, rather than a shear strain on the twinning plane. When a precipitate is partially engulfed by a twin, the portion in the parent and the portion in the twin experience different strain state, giving rise to the deflection of the precipitate. Such deflection is purely elastic. When the precipitate is entirely engulfed by the twin, the difference in strain state vanishes and the deflection is recovered.
(3) During precipitate-TB interaction, the deflection of the precipitate can be inversed due to the fact that twinning causes relaxation to the precipitate, as a result of basal-prismatic transformation between the parent and the twin.

Acknowledgements

Bin Li gratefully thanks support from the U.S. National Science Foundation (NSF) (CMMI-1635088).

References

[1] Q. Yu, J. Wang, Y. Jiang, R.J. McCabe, N. Li, C.N. Tomé, Twin–twin interactions in magnesium, Acta Mater. 77 (2014) 28–42, https://doi.org/10.1016/j.actamat.2014.05.030.
[2] C. Frank, Magnesium Alloys-Design, Processing and Properties, Intech, India, 2011.
[3] T.M. Pollock, Weight loss with magnesium alloys, Science 328 (2010) 986–987.
[4] J.-F. Nie, Precipitation and Hardening in Magnesium Alloys, Metall. Mater. Trans. A 43 (2012) 3891–3939, https://doi.org/10.1007/s11661-012-1217-2.
[5] P. Chen, B. Li, D. Culbertson, Y. Jiang, Negligible effect of twin-slip interaction on hardening in deformation of a Mg-3Al-1Zn alloy, Mater. Sci. Eng. A. (n.d.). http://doi.org/10.1016/j.msea.2018.05.067.
[6] P. Chen, B. Li, D. Culbertson, Y. Jiang, Contribution of extension twinning to plastic strain at low stress stage deformation of a Mg-3Al-1Zn alloy, Mater. Sci. Eng. A 709 (2018) 40–45, https://doi.org/10.1016/j.msea.2017.10.038.
[7] C.R. Hutchinson, J.-F. Nie, S. Gorsse, Modeling the precipitation processes and strengthening mechanisms in a Mg-Al-(Zn) AZ91 alloy, Metall. Mater. Trans. A 36 (2005) 2093–2105.
[8] J.D. Robson, N. Stanford, M.R. Barnett, Effect of precipitate shape on slip and twinning in magnesium alloys, Acta Mater. 59 (2011) 1945–1956, https://doi.org/10.1016/j.actamat.2010.11.060.
[9] N. Stanford, J. Geng, Y.B. Chun, C.H.J. Davies, J.F. Nie, M.R. Barnett, Effect of plate-shaped particle distributions on the deformation behaviour of magnesium alloy AZ91 in tension and compression, Acta Mater. 60 (2012) 218–228, https://doi.org/10.1016/j.actamat.2011.10.001.
[10] M.R. Barnett, Twinning and the ductility of magnesium alloys, Mater. Sci. Eng. A 464 (2007) 1–7, https://doi.org/10.1016/j.msea.2006.12.037.
[11] J.W. Christian, S. Mahajan, Deformation twinning, Prog. Mater. Sci. 39 (1995) 1–157.
[12] J.W. Christian, The Theory of Transformations in Metals and Alloys. Pt. 2: [...], 3 ed., Pergamon, Amsterdam, 2002.

[13] M.Z. Bian, K.S. Shin, {10-12}twinning behavior in magnesium single crystal, Met. Mater. Int. 19 (2013) 999–1004, https://doi.org/10.1007/s12540-013-5012-4.
[14] J.P. Hirth, J. Lothe, Theory of dislocations, 1982.
[15] J.B. Clark, Age hardening in a Mg-9 wt.% Al alloy, Acta Metall. 16 (1968) 141–152, https://doi.org/10.1016/0001-6160(68)90109-0.
[16] S. Celotto, TEM study of continuous precipitation in Mg–9 wt%Al–1 wt%Zn alloy, Acta Mater. 48 (2000) 1775–1787, https://doi.org/10.1016/S1359-6454(00)00004-5.
[17] A.F. Crawley, K.S. Milliken, Precipitate morphology and orientation relationships in an aged Mg-9% Al-1% Zn-0.3% Mn alloy, Acta Metall. 22 (1974) 557–562, https://doi.org/10.1016/0001-6160(74)90152-7.
[18] M. Zhang, F. Ye, W.-Z. Zhang, Interpretation of precipitation crystallography of Mg17Al12 in a Mg-Al alloy in terms of singular interfacial structure, Metall. Mater. Trans. A 36 (2005) 1681–1688.
[19] M.-X. Zhang, P.M. Kelly, Crystallography of Mg17Al12 precipitates in AZ91D alloy, Scr. Mater. 48 (2003) 647–652, https://doi.org/10.1016/S1359-6462(02)00555-9.
[20] J.F. Nie, Effects of precipitate shape and orientation on dispersion strengthening in magnesium alloys, Scr. Mater. 48 (2003) 1009–1015, https://doi.org/10.1016/S1359-6462(02)00497-9.
[21] M. Liao, B. Li, M.F. Horstemeyer, Interaction between prismatic slip and a Mg17Al12 precipitate in magnesium, Comput. Mater. Sci. 79 (2013) 534–539, https://doi.org/10.1016/j.commatsci.2013.07.016.
[22] M. Liao, B. Li, M.F. Horstemeyer, Interaction between basal slip and a Mg17Al12 precipitate in magnesium, Metall. Mater. Trans. A 45 (2014) 3661–3669, https://doi.org/10.1007/s11661-014-2284-3.
[23] J.D. Robson, N. Stanford, M.R. Barnett, Effect of precipitate shape and habit on mechanical asymmetry in magnesium alloys, Metall. Mater. Trans. A 44 (2013) 2984–2995, https://doi.org/10.1007/s11661-012-1466-0.
[24] N. Stanford, M.R. Barnett, Effect of particles on the formation of deformation twins in a magnesium-based alloy, Mater. Sci. Eng. A 516 (2009) 226–234, https://doi.org/10.1016/j.msea.2009.04.001.
[25] M.A. Gharghouri, G.C. Weatherly, J.D. Embury, The interaction of twins and precipitates in a Mg-7.7 at.% Al alloy, Philos. Mag. A 78 (1998) 1137–1149, https://doi.org/10.1080/01418619808239980.
[26] J.B. Clark, Transmission electron microscopy study of age hardening in a Mg-5 wt.% Zn alloy, Acta Metall. 13 (1965) 1281–1289.
[27] J. Jain, W.J. Poole, C.W. Sinclair, M.A. Gharghouri, Reducing the tension–compression yield asymmetry in a Mg–8Al–0.5Zn alloy via precipitation, Scr. Mater. 62 (2010) 301–304, https://doi.org/10.1016/j.scriptamat.2009.11.024.
[28] B.-Y. Liu, N. Yang, J. Wang, M. Barnett, Y.-C. Xin, D. Wu, R.-L. Xin, B. Li, R.L. Narayan, J.-F. Nie, J. Li, E. Ma, Z.-W. Shan, Insight from in situ microscopy into which precipitate morphology can enable high strength in magnesium alloys, J. Mater. Sci. Technol. (2018), https://doi.org/10.1016/j.jmst.2018.01.017.
[29] J. Wang, N. Stanford, Investigation of precipitate hardening of slip and twinning in Mg5%Zn by micropillar compression, Acta Mater. 100 (2015) 53–63, https://doi.org/10.1016/j.actamat.2015.08.012.
[30] B. Li, S.N. Mathaudhu, Interaction between a Mg17Al12 precipitate and {1012} < 10Ï2 > twin boundary in magnesium alloys, Magnes. Technol. 6 (2013).
[31] B. Li, X.Y. Zhang, Twinning with zero twinning shear, Scr. Mater. 125 (2016) 73–79, https://doi.org/10.1016/j.scriptamat.2016.07.004.
[32] J. Geng, Y.B. Chun, N. Stanford, C.H.J. Davies, J.F. Nie, M.R. Barnett, Processing and properties of Mg–6Gd–1Zn–0.6Zr: Part 2. Mechanical properties and particle twin interactions, Mater. Sci. Eng. A 528 (2011) 3659–3665, https://doi.org/10.1016/j.msea.2011.01.024.
[33] M.I. Baskes, Modified embedded-atom potentials for cubic materials and impurities, Phys. Rev. B 46 (1992) 2727–2742, https://doi.org/10.1103/PhysRevB.46.2727.
[34] X.-Y. Liu, J.B. Adams, F. Ercolessi, J.A. Moriarty, EAM potential for magnesium from quantum mechanical forces, Model. Simul. Mater. Sci. Eng. 4 (1996) 293, https://doi.org/10.1088/0965-0393/4/3/004.
[35] X.-Y. Liu, P.P. Ohotnicky, J.B. Adams, C.L. Rohrer, R.W. Hyland, Anisotropic surface segregation in Al-Mg alloys, Surf. Sci. 373 (1997) 357–370.
[36] A. Stukowski, Visualization and analysis of atomistic simulation data with OVITO–the Open Visualization Tool, Model. Simul. Mater. Sci. Eng. 18 (2010) 015012.
[37] B. Li, E. Ma, Atomic shuffling dominated mechanism for deformation twinning in magnesium, Phys. Rev. Lett. 103 (2009) 035503.
[38] F. Wang, B. Li, Surface and interfacial energies of Mg17Al12–Mg system, in: D. Orlov, V. Joshi, K.N. Solanki, N.R. Neelameggham (Eds.), Magnes. Technol. Springer International Publishing, 2018, pp. 55–62.
[39] B.-Y. Liu, J. Wang, B. Li, L. Lu, X.-Y. Zhang, Z.-W. Shan, J. Li, C.-L. Jia, J. Sun, E. Ma, Twinning-like lattice reorientation without a crystallographic twinning plane, Nat. Commun. 5 (2014).
[40] J.D. Honeycutt, H.C. Andersen, Molecular dynamics study of melting and freezing of small Lennard-Jones clusters, J. Phys. Chem. 91 (1987) 4950–4963, https://doi.org/10.1021/j100303a014.
[41] D. Faken, H. Jónsson, Systematic analysis of local atomic structure combined with 3D computer graphics, Comput. Mater. Sci. 2 (1994) 279–286, https://doi.org/10.1016/0927-0256(94)90109-0.
[42] M.R. Barnett, Twinning super dislocations to help understand strength, in: K.N. Solanki, D. Orlov, A. Singh, N.R. Neelameggham (Eds.), Magnes Technol. Springer International Publishing, Cham, 2017, pp. 143–145, , https://doi.org/10.1007/978-3-319-52392-7_22.
[43] J. Friedel, Dislocations, 1964, Oxford. 70 (n.d.) 15–24.
[44] J. Gil, Sevillano, Geometrically necessary twins and their associated size effects, Scr. Mater. 59 (2008) 135–138, https://doi.org/10.1016/j.scriptamat.2008.02.052.
[45] J.D. Robson, The effect of internal stresses due to precipitates on twin growth in magnesium, Acta Mater. 121 (2016) 277–287, https://doi.org/10.1016/j.actamat.2016.09.022.
[46] J.D. Eshelby, The determination of the elastic field of an ellipsoidal inclusion, and related problems, Proc. R. Soc. Lond. A 241 (1957) 376–396.
[47] J.D. Eshelby, The elastic field outside an ellipsoidal inclusion, Proc. R. Soc. Lond. A 252 (1959) 561–569.
[48] J. Eshelby, Elastic inclusions and inhomogeneities, Prog. Solid Mech. 2 (1961) 89–140.
[49] H. Fan, Y. Zhu, J.A. El-Awady, D. Raabe, Precipitation hardening effects on extension twinning in magnesium alloys, Int. J. Plast. 106 (2018) 186–202, https://doi.org/10.1016/j.ijplas.2018.03.008.
[50] M.H. Yoo, Slip, twinning, and fracture in hexagonal close-packed metals, Metall. Trans. A 12 (1981) 409–418, https://doi.org/10.1007/BF02648537.
[51] Y. Zhang, Z.S. Dong, J.T. Wang, J.Q. Liu, N. Gao, T.G. Langdon, An analytical approach and experimental confirmation of dislocation–twin boundary interactions in titanium, J. Mater. Sci. 48 (2013) 4476–4483, https://doi.org/10.1007/s10853-013-7284-y.
[52] B. Li, X.Y. Zhang, Global strain generated by shuffling-dominated {10$\bar{1}$2} < 10$\bar{1}$ $\bar{1}$ > twinning, Scr. Mater. 71 (2014) 45–48, https://doi.org/10.1016/j.scriptamat.2013.10.002.
[53] X.Y. Zhang, B. Li, J. Tu, Q. Sun, Q. Liu, Non-classical twinning behavior in dynamically deformed cobalt, Mater. Res. Lett. 3 (2015) 142–148, https://doi.org/10.1080/21663831.2015.1034297.
[54] J. Wang, I.J. Beyerlein, Atomic structures of symmetric tilt grain boundaries in hexagonal close packed (hcp) crystals, Model. Simul. Mater. Sci. Eng. 20 (2012) 024002, , https://doi.org/10.1088/0965-0393/20/2/024002.
[55] C. Cayron, Hard-sphere displacive model of extension twinning in magnesium, Mater. Des. 119 (2017) 361–375, https://doi.org/10.1016/j.matdes.2017.01.047.
[56] C. Cayron, Shifting the shear paradigm in the crystallographic models of displacive transformations in metals and alloys, Crystals 8 (2018) 181, https://doi.org/10.3390/cryst8040181.
[57] J. Jain, P. Cizek, W.J. Poole, M.R. Barnett, The role of back stress caused by precipitates on {10$\bar{1}$2} twinning in a Mg–6Zn alloy, Mater. Sci. Eng. A 647 (2015) 66–73, https://doi.org/10.1016/j.msea.2015.08.091.